Journal of
Experimental and Theoretical Analyses

MDPI

Article

Thermal Performance of Silicone and Non-Silicone Thermal Pads as Thermal Interface Materials

Chandan Roy *, Landon Yarbrough, Hammad Quddus and Megan Batchelor

Mechanical Engineering, Mercer University, 1501 Mercer University Drive, Macon, GA 31207, USA; landon.james.yarbrough@live.mercer.edu (L.Y.); hammad.afzal.quddus@live.mercer.edu (H.Q.); megan.elizabeth.batchelor@live.mercer.edu (M.B.)
* Correspondence: roy_ck@mercer.edu

Abstract

The research presents the thermal performance comparison of silicone and non-silicone thermal pads using a steady-state thermal interface material (TIM) testing apparatus. The TIM tester follows standard guidelines for testing thermal properties. TIMs are applied between two solid surfaces to improve heat transfer by eliminating air gaps that naturally occur due to surface roughness and non-flatness. Since TIMs possess significantly higher thermal conductivity than air, they effectively reduce contact resistance at the interface, thereby minimizing the risk of overheating in electronic systems. In this work, the thermal resistances of silicone and non-silicone thermal pads were compared over a pressure range of 10–50 psi. Results indicate that non-silicone pads consistently exhibit lower thermal resistance than their silicone counterparts under identical testing conditions.

Keywords: thermal interface material; thermal resistance; thermal pad; heat transfer

check for updates

Academic Editor: Marco Rossi

Received: 7 August 2025
Revised: 5 September 2025
Accepted: 16 September 2025
Published: 5 October 2025

Citation: Roy, C.; Yarbrough, L.; Quddus, H.; Batchelor, M. Thermal Performance of Silicone and Non-Silicone Thermal Pads as Thermal Interface Materials. *J. Exp. Theor. Anal.* **2025**, *3*, 30. https://doi.org/10.3390/jeta3040030

Copyright: © 2025 by the authors. Licensee MDPI, Basel, Switzerland. This article is an open access article distributed under the terms and conditions of the Creative Commons Attribution (CC BY) license (https://creativecommons.org/licenses/by/4.0/).

1. Introduction

As computers and electronic devices continue to become smaller, faster, and more powerful, efficient thermal management has emerged as one of the most pressing challenges in modern electronics. Increasing power densities result in greater heat generation, which must be dissipated effectively to ensure device reliability and prevent thermal failure. Heat sinks, with their extended finned geometries, are widely employed to enhance cooling; however, before heat can be transferred to the surrounding environment, it must first be conducted from the heat-generating component to the heat sink. Where the heat source meets the heat sink, there are minuscule air-filled gaps due to the roughness of these surfaces at the microscopic level [1–3], as shown in Figure 1. Due to the low thermal conductivity of air (0.026 W/m·K) [3], these gaps reduce the amount of heat transfer from the source to the sink, resulting in additional resistance to heat flow, known as thermal contact resistance [1–3].

One way to reduce the thermal contact resistance is by filling the gap with a highly conductive material, known as a thermal interface material (TIM) [1–3]. The TIM increases the number of contact points between the two surfaces, allowing more heat to be conducted across the interface [3]. When a TIM is added, there is still a contact resistance between the surface and the TIM due to the microscopic roughness of the surface; however, the overall thermal interface resistance is reduced significantly. A magnified view of an imperfect contact with TIM is shown in Figure 2.

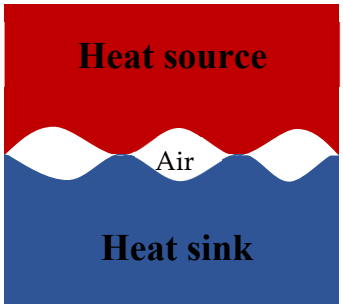


Figure 1. A magnified contact between the heat source and heat sink with air at the interface.

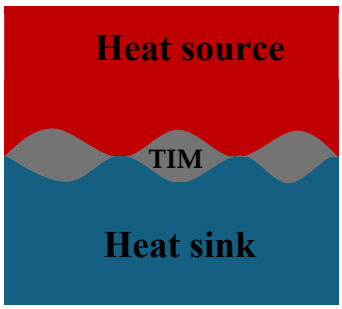


Figure 2. A magnified contact between the heat source and heat sink with TIM at the interface.

There are many different types of TIMs, including thermal pads, thermal grease, phase change materials, liquid metal alloys, and carbon nanotubes [3–8]. Each type of TIM has different properties with different advantages and disadvantages. This study compares the thermal performance of silicone-based and non-silicone thermal pads under a pressure range of 10–50 psi, which is typical for electronics cooling applications [3].

Thermal gap pads are a class of TIMs designed to fill air gaps and ensure effective heat transfer between electronic components and heat spreaders or heat sinks. Thermal gap pads are typically made from silicone or non-silicone polymer matrices embedded with thermally conductive fillers such as ceramic particles or graphite. Their soft, compliant nature allows them to fill uneven surfaces and air gaps, thereby minimizing interfacial thermal resistance [9]. Unlike thermal greases, which can suffer from issues like pump-out and drying over time, thermal gap pads offer long-term mechanical stability and are easier to handle and rework during assembly processes [10].

Silicone-based thermal gap pads are the most widely used due to their high flexibility, thermal stability, and ability to conform to surface irregularities [4]. These pads typically consist of a silicone elastomer matrix embedded with thermally conductive fillers such as alumina, boron nitride, or graphite [11]. Their inherent softness allows them to compress easily, minimizing interfacial resistance and enhancing heat dissipation. Moreover, silicone pads offer long-term reliability, maintaining performance over extended thermal cycling [10]. However, silicone migration (also known as outgassing or "bleed-out") can be a concern, particularly in optoelectronic or disk-drive applications where contamination sensitivity is critical [12].

Non-silicone thermal gap pads have been developed to address contamination associated with silicone materials. These pads are often formulated from hydrocarbon-, urethane-, or acrylic-based polymers loaded with thermally conductive fillers [9]. Non-silicone pads provide similar levels of conformability and thermal conductivity but avoid issues related to volatile siloxane outgassing [12]. As a result, they are especially suitable for applications in telecommunications, automotive electronics, and optical devices, where silicone contamination could compromise performance.

2. Materials and Methods

The materials chosen for this research were silicone and non-silicone thermal pads of the same nominal thickness and thermal conductivity. Table 1 shows the properties of silicone and non-silicone thermal pads that were purchased from DigiKey (Thief River Falls, MN 56701, USA, manufacturer: Shiu Li Technology, LLC). The goal was to compare the thermal resistances at different pressures.

Table 1. Properties of silicone and non-silicone thermal pads.

Property	Silicone Pad	Non-Silicone Pad
Thermal conductivity (W/m·K)	11	11
Nominal thickness (mm)	1	1
Density (g/cm^3)	3.4	3.3
Hardness	65	50

To evaluate the thermal performance of TIMs, a steady-state thermal setup has been used widely [1–3]. For this research purpose, a steady-state thermal test setup was designed and built as shown in Figure 3. The design followed the guidelines outlined in the ASTM D5470 standard [13]. The test apparatus consisted of two vertically aligned meter bars made of aluminum 6061 T6 alloy purchased from Online Metals (onlinemetals.com, location: Acworth, GA 30102, USA). The meter bar testing section was round with a diameter of 3.3 cm (1.3 in). The top meter bar was hot, and the bottom one functioned as cold. One-dimensional heat flow through the meter bar was maintained by minimizing lateral losses using proper insulation. The thermal resistance of the TIM was calculated based on fundamental heat transfer principles by measuring the temperature gradients along the meter bars and the applied heat flow.

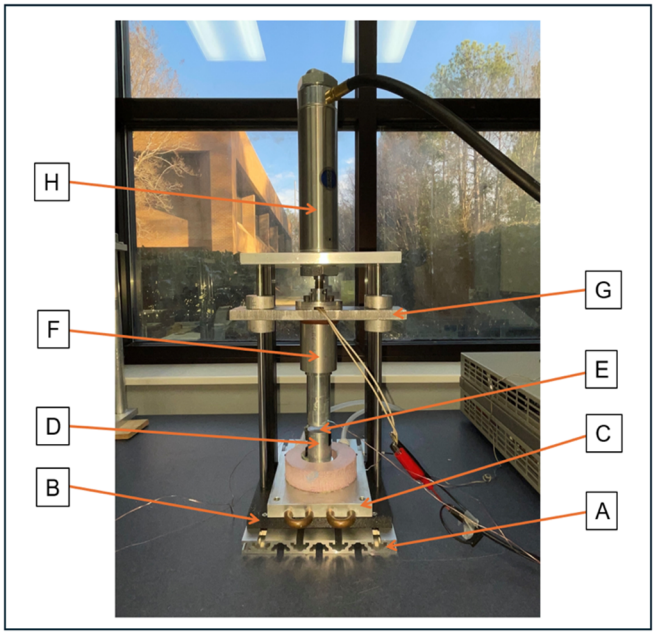


Figure 3. The experimental setup without insulation wrapped around the meter bar A. Aluminum base plate B. 3-D printed plate C. Aluminum cold plate D. Bottom half of meter bar E. TIM insertion space F. Top half of meter bar G. Vertically sliding plate H. Compressed air cylinder.

The top meter bar contained three thermocouple holes, while the bottom bar included two for precise temperature measurement at the interface. A cartridge heating element was embedded in the top meter bar. The heater was powered by a DC power supply. The bottom

meter bar is mounted on a cooling plate, which is connected to a recirculating chiller. Water flows through two inlet and outlet pipes to maintain an isothermal boundary condition.

Structural support was provided by two vertical cylindrical columns on either side of the setup. A rectangular aluminum plate was placed on top of the heater and bolted to these columns. Compressive force was applied using a pneumatic air cylinder mounted above this plate, delivering adjustable pressure up to 100 psi via a regulated air hose and pressure gauge. The accuracy of the pressure gauge was ±2 psi. To stabilize the assembly, a second aluminum plate was bolted to the top of the columns. After applying the desired pressure, appropriate insulation was wrapped around the meter bars to ensure accurate and consistent heat flow measurements.

The thermal pad was cut into a 3.3 cm round sample using a sample cutter and was placed between the two meter bars, after which the top meter bar was carefully lowered onto the bottom bar. Any excess TIM was removed to ensure clean contact surfaces. Once aligned, the desired pressure was applied, and insulation was wrapped around the meter bars to minimize heat loss. Electrical power was then supplied to the heater embedded in the top meter bar, initiating heat flow through the TIM. Heat was conducted in a one-dimensional path toward the bottom meter bar, which was maintained at a constant temperature by the cooling plate. Data collection began once the thermal steady-state condition was achieved as described by the standard [14].

Experimental Uncertainty Analysis

The uncertainty in thermal resistance was calculated using the root-sum-square method [15]. The calculated uncertainties in the measurement are represented by the error bar in all foregoing figures representing the thermal resistance of pads.

The thermal resistance of the TIM is given as follows:

$$R = \frac{\Delta T}{q}$$

where ΔT is the temperature drop across the interface, and q is the heat flow (equivalent to the applied electrical power, in Watts). The uncertainty in thermal resistance can be expressed as follows:

$$\frac{UR}{R} = \sqrt{\left(\frac{U\Delta T}{\Delta T}\right)^2 + \left(\frac{Uq}{q}\right)^2}$$

where $U\Delta T$ is the uncertainty in temperature measurement and Uq is the uncertainty in heat flow measurement. In all reported results, the following values were used: uncertainty in heat flow of ±10% and uncertainty in temperature measurement of ±0.2 °C (based on thermocouple accuracy).

3. Results

The tests were performed without any sample (called baseline tests) and using two types of thermal pads: silicone thermal pads and non-silicone thermal pads.

3.1. Baseline Tests

The purpose of these tests was to measure the thermal resistance without any TIM at the interface. If there is no TIM placed at the interface, most of the interfacial spaces are filled with air, which is a poor conductor of heat. The thermal resistance was expected to be high without any TIM at the interface. Tests were conducted at two different pressures, 20 and 50 psi, and the results are presented in Table 2. Results showed that with the increase in pressure, the thermal resistance decreased. This is because, with pressure, the meter bar

surfaces make better contact, and more air is displaced from the interface. These baseline tests with high thermal resistances justify the importance of using a TIM at the interface to enhance heat transfer.

Table 2. Thermal resistance of bare interface (without any TIM) at different applied pressures.

Pressure (psi)	Thermal Resistance (K/W)
20	0.64
50	0.53

3.2. Testing of Silicone Thermal Pad

A silicone thermal pad of thermal conductivity 11 W/m·K was chosen for the test. The tests were performed at different pressures ranging from 10 to 50 psi. For all tests, the temperature at the interface was maintained at 50 °C ± 2. Figure 4 represents the thermal resistance at various applied pressures. The pad offers lower thermal resistance (better heat transfer) when compared to tests without any TIM. At the same pressure of 20 psi, the thermal resistance of the silicone pad is about 85% lower than the baseline test. This result emphasizes the importance of using TIM at the interface. With the silicone pad, the thermal resistance decreased by about 63% as the pressure increased from 10 to 50 psi. As the pressure increases, the TIM materials make better contact with the matting surfaces by displacing more air gaps from the interface, thereby reducing the contact resistance. Also, these are soft elastomeric pads, which deform under pressure. With increasing pressure, the thickness decreases, which in turn reduces the conduction resistance. Combining these two effects, the overall thermal resistance decreases with increasing pressure.

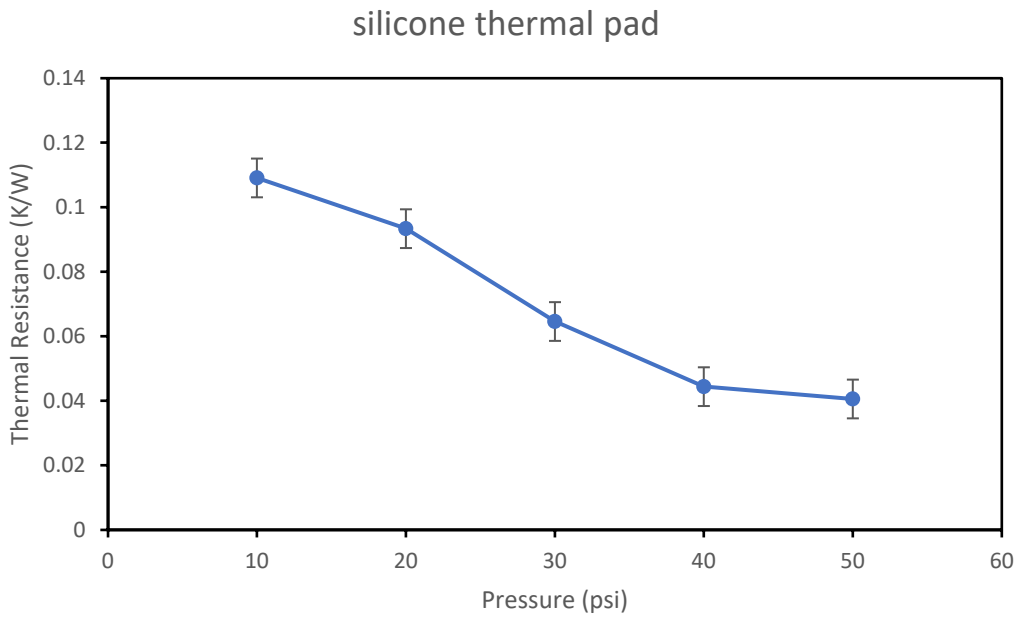


Figure 4. Thermal resistance of a silicone thermal pad at various pressures.

3.3. Testing of Non-Silicone Thermal Pad

A non-silicone thermal pad of the same thermal conductivity as the silicone thermal pad (11 W/m·K) was chosen for the test. The non-silicone pad is made by silicone-free resin materials. Again, similar to the silicone pad, the tests were performed at various pressures, and the thermal resistance values are shown in Figure 5. A similar trend was observed: thermal resistances decreased by about 47% with the increase of pressure from 10 to 50 psi. This behavior was expected and, for the same reason, is explained in the previous section.

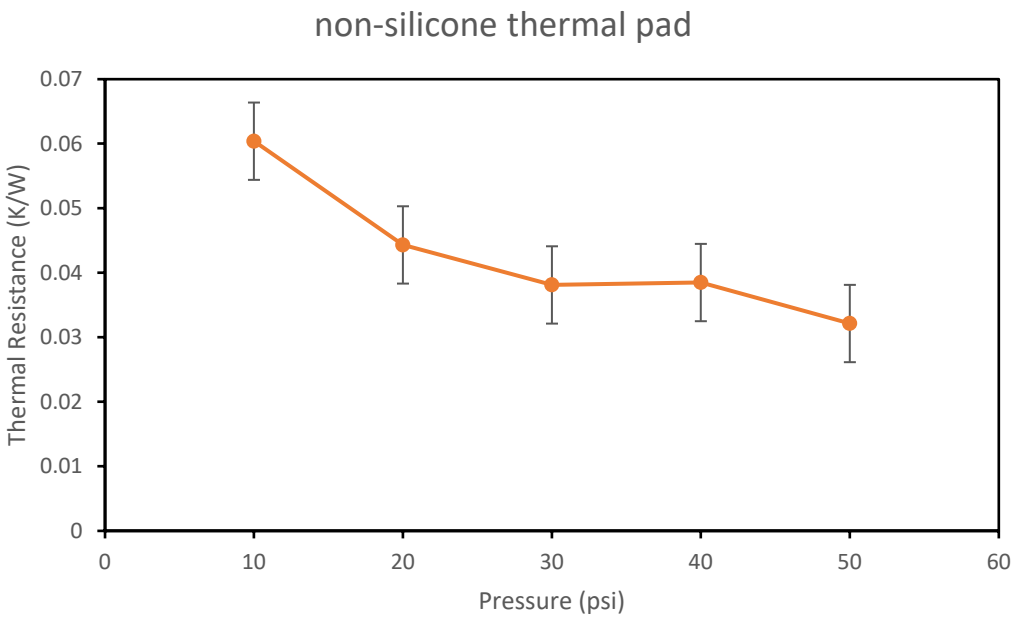


Figure 5. Thermal resistance of a non-silicone thermal pad at various pressures.

3.4. Performance Comparison

Figure 6 shows the performance comparison of the thermal resistance of silicone and non-silicone thermal pads. Even though both of them have the same conductivity and the same initial thickness, the thermal resistance differs. At all pressures in the range 10–50 psi, the non-silicone pad offers better thermal performance (lower thermal resistances) compared to the silicone thermal pad. At pressures of about 40 psi and above, both pads offer similar thermal performance (within the experimental uncertainty).

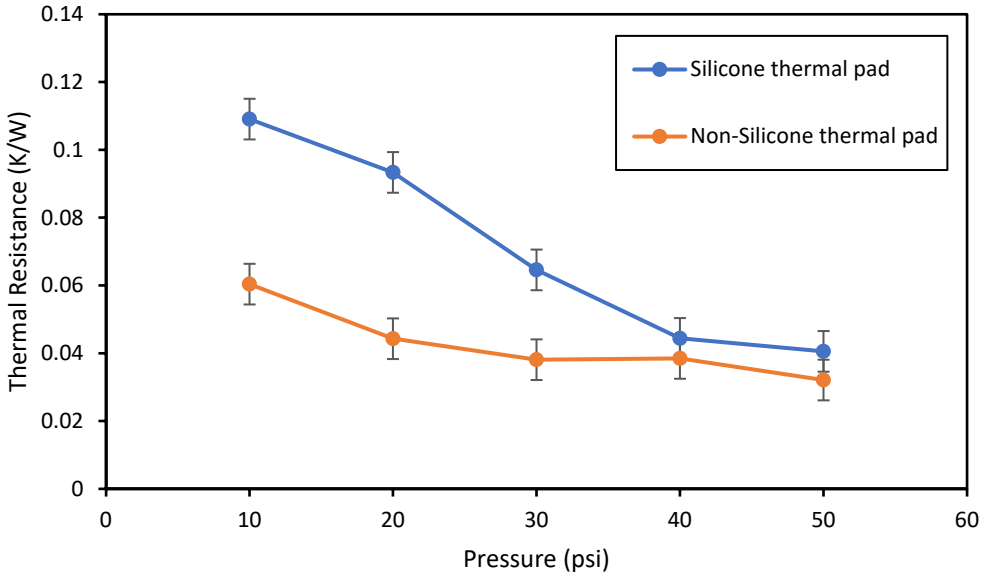


Figure 6. Thermal resistance comparison of silicone and non-silicone thermal pad at various pressures.

3.5. Test Results Repeatability

To ensure repeatability, each test was performed three times at the same applied pressure. For each trial, the system was allowed to reach steady-state temperatures before data collection. Afterward, the heater was turned off, the pressure was released, and the system was cooled for 15 min while the cold plate continued to operate. The heater was then reactivated, pressure was reapplied, and steady-state temperatures were recorded again.

This procedure was repeated for a total of three tests. Throughout all trials, the power input from the power supply and the cold plate temperature were maintained constant. The relative standard deviation (RSD) of the three measurements was approximately 3%, confirming the excellent repeatability of the test results.

4. Discussion

It is known that the total thermal resistance of a pad consists of conduction resistance (derived from the thickness and thermal conductivity) and two contact resistances at the interface. Non-silicone pads often show better wetting or adhesion to surfaces than silicone pads. This improves the real contact area, reducing the microscopic voids filled with air, which leads to lower contact resistance. Silicone pads can exhibit oil bleed-out or outgassing, which may slightly alter their surface contact quality over time [12]. Non-silicone pads are designed specifically to avoid this, which may lead to more stable and lower initial contact resistance. In addition, thermal pads must deform to fill surface asperities. Even at the same nominal thickness, silicone pads tend to be more elastic (spring back), while non-silicone pads are often more plastically compliant. Non-silicone pads may conform more permanently under pressure, reducing micro-gaps and thereby lowering interface resistance. Both pad types use conductive fillers to enhance the thermal conductivity. In non-silicone systems, the polymer–filler interaction and pad microstructure sometimes lead to better particle packing at the interface, enhancing thermal pathways compared to silicone matrices.

Blazej (2003) reported that the thermal resistance of elastomeric thermal interface pads typically falls within the range of 1–3 $cm^2 \cdot K/W$ [4]. Wasniewski et al. [6] observed a decrease in the thermal resistance of the Bergquist Gap Pad 5000S35 from 0.84 to 0.81 $cm^2 \cdot K/W$ as the applied pressure increased from 20 to 50 psi. Similarly, Roy et al. [15] reported values for the same pad ranging from 0.98 to 0.90 $cm^2 \cdot K/W$ over the same pressure range. In the same study, Roy et al. also found that the thermal resistance of the Bergquist Sil Pad A2000 decreased from 1.85 to approximately 1.65 $cm^2 \cdot K/W$ under increasing pressure from 20 to 50 psi. Deng and Jiang (2021) [16] reported a thermal resistance of 1.17 $cm^2 \cdot K/W$ at 50 psi for the Laird Tflex 720 thermal pad. Furthermore, they developed a novel soft-metal thermal pad that exhibited a thermal resistance of 0.59 $cm^2 \cdot K/W$ before surface treatment, which was further reduced to 0.15 $cm^2 \cdot K/W$ after treatment, both measured at 50 psi.

For comparison, the tested silicone pad in this work exhibited a thermal resistance of 0.80–0.35 $cm^2 \cdot K/W$, while the non-silicone pad showed a range of 0.38–0.28 $cm^2 \cdot K/W$ within the pressure range from 20 to 50 psi. According to manufacturer specifications, the thermal conductivities of the pads are 5.0 $W/m \cdot K$ for the Bergquist Gap Pad 5000S35, 3 $W/m \cdot K$ for the Bergquist Sil Pad A2000, and 5 $W/m \cdot K$ for Larid Tflex 720. In contrast, both of the tested silicone and non-silicone pads had significantly higher thermal conductivities of 11 $W/m \cdot K$. The enhanced thermal performance, reflected in reduced thermal resistance, can be attributed to the superior thermal conductivity and improved surface adhesion characteristics of the tested materials.

5. Conclusions

In this study, the thermal performance of silicone and non-silicone thermal pads of the same thickness and conductivity was tested using a steady-state thermal test setup. Results show that the thermal pad reduces thermal resistance significantly at the interface when compared to no TIM placed. This result justifies the benefit of using a TIM at the interface whenever heat transfer is concerned. In all cases (with and without thermal pad), the thermal resistance decreases with increasing pressure. Comparing the thermal resistance of silicone and non-silicone pads, the non-silicone pad offers superior thermal performance

in the pressure range of 10–50 psi. Regarding sample preparation and handling, the silicone pad was easy to apply and remove, whereas the non-silicone pad, being softer (lower hardness value) and slightly tacky, required additional effort during application and removal.

In general, thermal pads are effective in conforming to surface irregularities, filling microscopic air gaps, and thereby reducing thermal contact resistance. Unlike thermal pastes, they are solid, preformed, and easy to handle, apply, and remove without creating a mess. Moreover, thermal pads avoid common issues associated with greases, such as "pump-out" and "dry-out". Their electrical insulation properties and wide range of available thermal conductivities make them suitable for various electronic cooling applications.

The silicone-based thermal pads can be used between the CPU and the heat sink, flat-panel displays, power supplies, high-speed mass storage drives, telecommunication equipment, 5G base stations and infrastructure, and high-performance semiconductor chips. Non-silicone thermal pads, on the other hand, are preferred in environments where silicone contamination must be avoided. The typical applications of non-silicone thermal pads include high-speed mass storage drives, optical systems and appliances, 5G base stations and infrastructure, and EV electric vehicles.

Author Contributions: Conceptualization, C.R.; methodology, C.R., L.Y., H.Q., M.B.; software, C.R., L.Y., H.Q.; validation, C.R.; formal analysis, C.R.; investigation, C.R., L.Y., H.Q., M.B.; resources, C.R., L.Y., H.Q., M.B.; data curation, C.R.; writing—original draft preparation, C.R.; writing—review and editing, C.R.; visualization, C.R.; supervision, C.R.; project administration, C.R. All authors have read and agreed to the published version of the manuscript.

Funding: This research received no external funding.

Data Availability Statement: The original contributions presented in this study are included in the article. Further inquiries can be directed to the corresponding author.

Conflicts of Interest: The authors declare no conflicts of interest.

Abbreviations

The following abbreviations are used in this manuscript:

TIM	Thermal Interface Material
ASTM	American Society for Testing and Materials

References

1. Zhao, J.; Zhao, R.; Huo, Y.; Cheng, W. Effects of Surface Roughness, Temperature and Pressure on Interface Thermal Resistance of Thermal Interface Materials. *Int. J. Heat Mass Transf.* **2019**, *140*, 705–716. [CrossRef]
2. Prasher, R. Thermal Interface Materials: Historical Perspective, Status, and Future Directions. *Proc. IEEE* **2006**, *94*, 1571–1586. [CrossRef]
3. Gwinn, J.P.; Webb, R.L. Performance and Testing of Thermal Interface Materials. *Microelectron. J.* **2003**, *34*, 215–222. [CrossRef]
4. Blazej, D. Thermal Interface Materials. *Electron. Cool.* **2003**, *9*, 14–21.
5. Sim, L.; Ramanan, S.R.; Ismail, H.; Seetharamu, K.N.; Goh, T.J. Thermal Characterization of Al_2O_3 and ZnO Reinforced Silicone Rubber as Thermal Pads for Heat Dissipation Purposes. *Thermochim. Acta* **2005**, *430*, 155–165. [CrossRef]
6. Wasniewski, J.R.; Altman, D.H.; Hodson, S.L.; Fisher, T.S.; Bulusu, A.; Graham, S.; Cola, B.A. Characterization of Metallically Bonded Carbon Nanotube-Based Thermal Interface Materials Using a High Accuracy 1D Steady-State Technique. *J. Electron. Packag.* **2012**, *134*, 020901. [CrossRef]
7. Sarvar, F.; Whalley, D.C.; Conway, P.P. Thermal Interface Materials—A Review of the State of the Art. In Proceedings of the 2006 1st Electronic Systemintegration Technology Conference, Dresden, Germany, 5–7 September 2006; Volume 2, pp. 1192–1202.
8. Prasher, R.S.; Matayabas, J.C., Jr. Thermal Contact Resistance of Cured Gel Polymeric Thermal Interface Material. *IEEE Trans. Compon. Packag. Technol.* **2004**, *27*, 702–709. [CrossRef]

9. Rao, V.V.; Raju, P.; Kumar, V. Thermal Performance and Reliability of Polymer-Based Thermal Interface Materials. *Mater. Today Proc.* **2020**, *28*, 200–205.
10. Gauthier, R.; Wang, J.; Prasher, R. Thermal Interface Materials: A Brief Review of Design Characteristics and Materials. *IEEE Trans. Compon. Packag. Manuf. Technol.* **2017**, *7*, 1261–1273.
11. Wang, H.; Li, H.; Xu, J. A Review on Thermal Management Materials for Electronic Applications. *Appl. Therm. Eng.* **2019**, *147*, 841–856.
12. Kim, H.S.; Lee, D.H.; Lee, K.H. Evaluation of Silicone Outgassing and Its Impact on Optical and Electronic Devices. *Microelectron. Reliab.* **2016**, *65*, 185–191. [CrossRef]
13. *ASTM D5470-12*; Standard Test Method for Thermal Transmission Properties of Thermally Conductive Electrical Insulation Materials. Technical Report. ASTM International: West Conshohocken, PA, USA, 2012.
14. Carlberg, B.; Wang, T.; Fu, Y.; Liu, J.; Shangguan, D. Nanostructured Polymer–Metal Composite for Thermal Interface Material Applications. In Proceedings of the 58th Electronic Components and Technology Conference (ECTC 2008), Lake Buena Vista, FL, USA, 27–30 May 2008; IEEE: Piscataway, NJ, USA, 2008; pp. 191–197.
15. Roy, C.K.; Bhavnani, S.; Hamilton, M.; Johnson, W.R.; Knight, R.W.; Harris, D.K. Performance of Low Melt Alloys as Thermal Interface Materials. In Proceedings of the 31st Annual Semiconductor Thermal Measurement and Management Symposium (SEMI-THERM 2015), San Jose, CA, USA, 15–19 March 2015.
16. Deng, Y.; Jiang, Y. High-performance, safe, and reliable soft-metal thermal pad for thermal management of electronics. *Appl. Therm. Eng.* **2021**, *199*, 117555. [CrossRef]

Disclaimer/Publisher's Note: The statements, opinions and data contained in all publications are solely those of the individual author(s) and contributor(s) and not of MDPI and/or the editor(s). MDPI and/or the editor(s) disclaim responsibility for any injury to people or property resulting from any ideas, methods, instructions or products referred to in the content.